

Discovery of a Cannabinoid CB₂ Receptor Fluorescent Probe Based on a Pyridin-2-yl-benzyl-imidazolidine-2,4-dione Scaffold

Laura V. de Paus^{*a} 

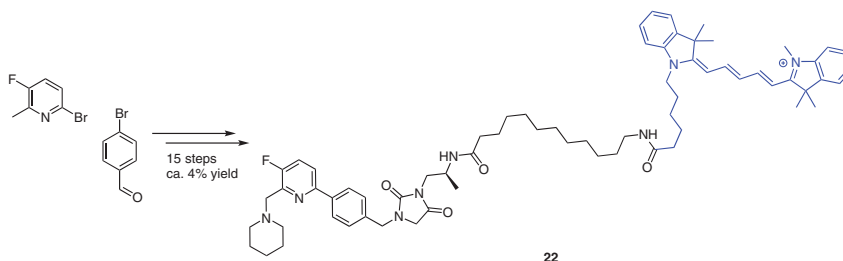
Antonius P.A. Janssen^a

Asad Halimi^a

Richard J. B. H. N. van den Berg^a

Laura H. Heitman^{b§}

Mario van der Stelt^{*a§}



^a Department of Molecular Physiology, LIC, Leiden University & Oncode Institute, Einsteinweg 55, 2333CC, Leiden, The Netherlands
L.v.de.paus@lic.leidenuniv.nl

^b Division of Drug Discovery and Safety, LACDR, Leiden University & Oncode Institute, Einsteinweg 55, 2333CC, Leiden, The Netherlands

§ Senior authors


Published as part of the Cluster
Japan/Netherlands Gratama Workshop

Received: 08.11.2023

Accepted after revision: 14.12.2023

Published online: 14.12.2023 (Accepted Manuscript), 30.01.2024 (Version of Record)

DOI: 10.1055/a-2230-1003; Art ID: ST-2023-10-0478-A

License terms: 

© 2024. The Author(s). This is an open access article published by Thieme under the terms of the Creative Commons Attribution License, permitting unrestricted use, distribution and reproduction, so long as the original work is properly cited. (<https://creativecommons.org/licenses/by/4.0/>)

Abstract Cannabinoid receptor type 2 (CB₂R) agonists have therapeutic potential for the treatment of (neuro)inflammatory diseases. Fluorescent probes enable the detection of CB₂R in relevant cell types and serve as a chemical tool in cellular target engagement studies. Here, we report the structure-based design and synthesis of a new CB₂R selective fluorescent probe. Based on the cryo-EM structure of LEI-102 in complex with the CB₂R, we synthesized 5-fluoropyridin-2-yl-benzyl-imidazolidine-2,4-dione analogues in which we introduced a variety of linkers and fluorophores. Molecular pharmacological characterization showed that compound **22**, containing a Cy5-fluorophore with an alkyl-spacer, was the most potent probe with a pK_i of 6.2 ± 0.6. It was selective over the cannabinoid CB₁ receptor and behaved as an inverse agonist (pEC₅₀ 5.3 ± 0.1, E_{max} -63% ± 6). Probe **22** may serve as a chemical tool in target and lead validation studies for the CB₂R.

Key words cannabinoid CB₂ receptor, fluorescent probes, LEI-102

The cannabinoid receptor type 2 (CB₂R) is a class A G protein-coupled receptor (GPCR) with a role in inflammation and neurodegenerative diseases, making it an interesting target for drug discovery for multiple applications.¹ Confirming target engagement and understanding the biological cascades that lead to the therapeutic effect of a therapeutic agent are necessary for the successful translation of compounds into the clinic. To date, no CB₂R-selective drugs have yet reached the market.² Fluorescent probes are ideal for detecting CB₂R in relevant cell types, target engagement studies and to explore the roles of CB₂R in healthy and

pathological systems.³ To this end, several fluorescent probes have been reported.^{2–14} We have also contributed to this field and reported 5-fluoropyridin-2-yl-benzyl-imidazolidine-2,4-dione LEI-121 (Figure 1A) as a CB₂R selective bifunctional probe that captured CB₂R upon photoactivation.¹⁵ An incorporated alkyne served as a ligation handle for the introduction of fluorescent reporter groups. LEI-121 enabled target engagement studies and visualization of endogenously expressed CB₂R in HL-60 and primary human immune cells using flow cytometry.¹⁵ However, LEI-121 is a two-step probe that requires copper-catalyzed azide-alkyne cycloaddition (click-reaction) with a fluorophore to visualize the receptor. For live imaging purposes, it would

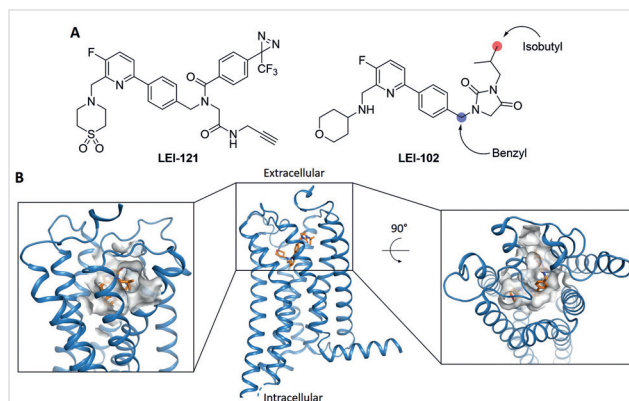


Figure 1 LEI-121 and LEI-102 and the resolved cryo-EM structure of hCB₂R with LEI-102. (A) The chemical structures of CB₂R probe LEI-121 and CB₂R agonist LEI-102. The optimal positions to attach a spacer are marked in the structure of LEI-102. (B) Cryo-EM structures of CB₂R (sky blue, PDB: 8GUT) in complex with LEI-102 (orange) at two different angles, with surface representation of receptor atoms within 4 Å. Figure generated with Open Source PyMOL Molecular Viewer v2.4.¹⁶

be beneficial to avoid the copper-mediated click reaction, which is toxic to cells, and to have a one-step fluorescent probe in which the fluorophore is incorporated into the structure of the ligand.

Previously, we have reported the three-dimensional structure of CB₂R in complex with the 5-fluoropyridin-2-yl-benzyl-imidazolidine-2,4-dione analogue LEI-102 using cryogenic electron microscopy (Figure 1).¹⁶ This provided an excellent opportunity for the structure-based design of novel one-step fluorescent CB₂R probes. To validate this reasoning, we set out to design, synthesize, and characterize novel one-step fluorescent CB₂R probes based on the 5-fluoropyridin-2-yl-benzyl-imidazolidine-2,4-dione series.

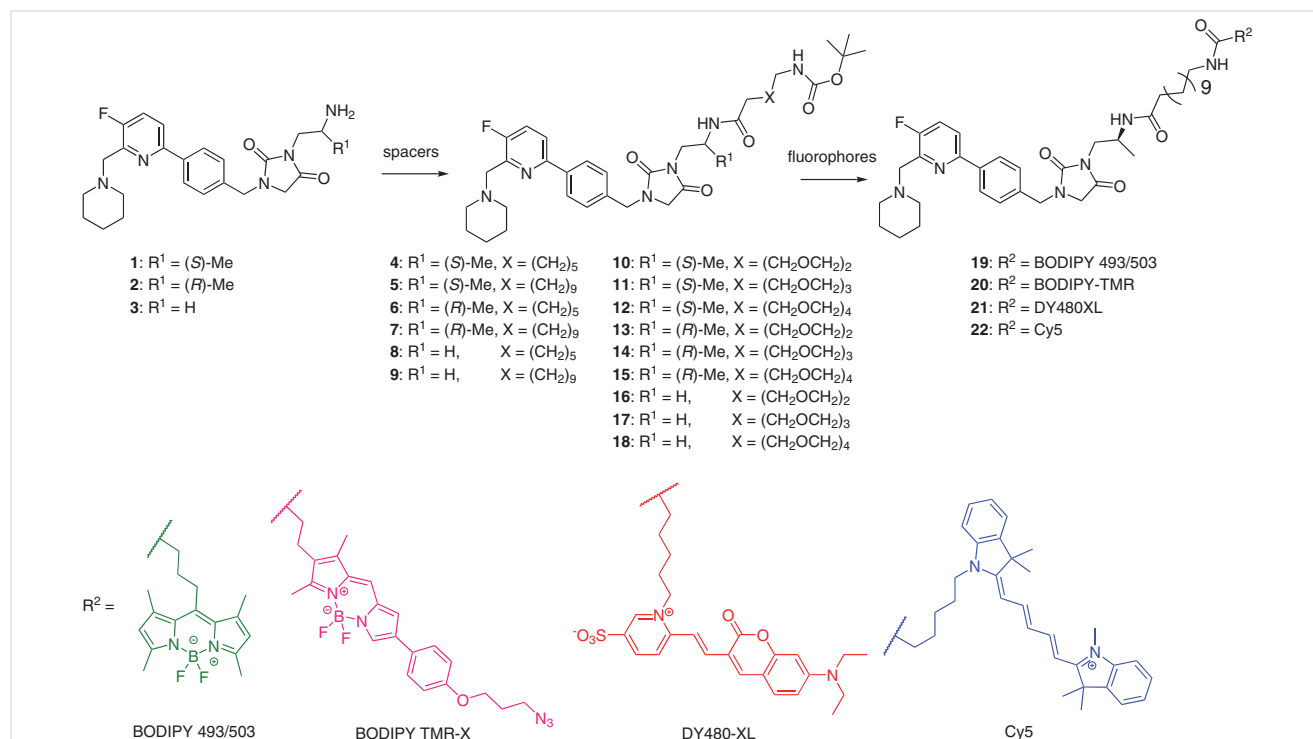
Design

The cryo-EM structure of human CB₂R in complex with LEI-102 was inspected to find the best exit vector on the scaffold for the introduction of a spacer that could be coupled to various fluorophores. The isobutyl and benzylic positions were positioned equally well to serve as an attachment point for spacer plus fluorophore. For synthetic reasons, the isobutyl position was chosen to introduce an optionally methyl substituted ethylamine (compounds **1–3**)

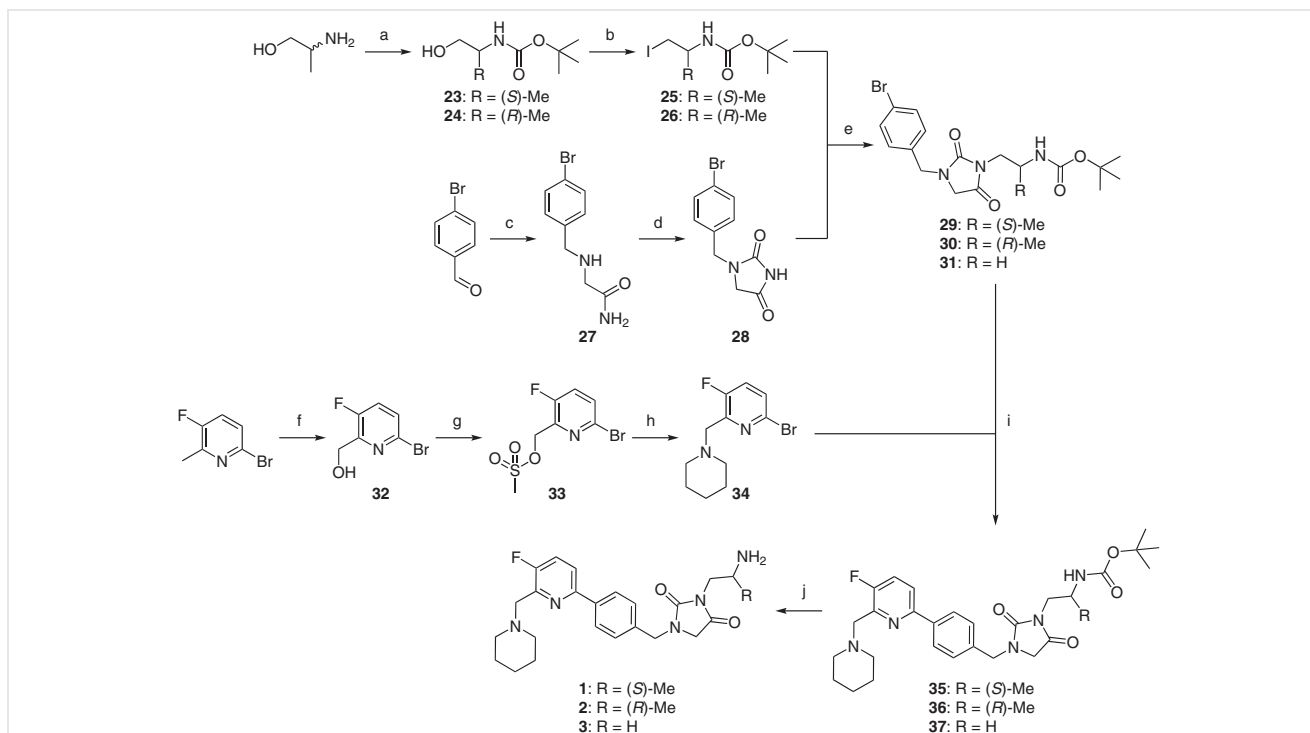
as attachment point for various alkyl (compounds **4–9**) or polyethylene glycol (PEG) (compounds **10–18**) spacers. The most promising scaffold-spacer compound (**5**) was coupled to four different fluorophores, i.e., BODIPY 493/503, BODIPY-TMR-X, DY480-XL, and Cy-5, resulting in compounds **19–22** (Scheme 1). BODIPY dyes have the advantages of high quantum yield, high molar extinction coefficients and brightness, as well as being relatively insensitive to the pH of their environment.^{17,18} Cy5 is frequently used and emits in the near-infrared range, which is not affected by biological auto-fluorescence, shows high stability, is moderately insensitive to solvent polarity, is highly water soluble, and has one of the highest molar extinction coefficients.^{19–21} DY-480XL has a large Stokes shift, which increases the signal-to-noise by lowering the chance of self-quenching, self-absorption, and excitation source cross-talk.²²

Synthesis

The synthesis²³ of the CB₂R-selective fluorescent probes based on LEI-102 **19–22** started with the construction of the pyridinylbenzylimidazolidine-2,4-dione intermediates **1–18**. Commercially available alaninol (D/L, Scheme 2) was carbamate protected (**23, 24**), then subsequent iodination



Scheme 1 The synthesis plan for the LEI-102-derived fluorescent probes. The scaffold contains an amine conjugation site that is either the (S)- or (R)-2-aminopropyl enantiomer or achiral 2-aminoethyl moiety. To all three scaffolds a selection of five spacers was conjugated: C₈, C₁₂, PEG₂, PEG₃, or PEG₄. Compound **5** exhibited the highest CB₂R affinity and was conjugated to the four fluorophores. The Cy5 conjugate **22** showed the best biochemical properties.

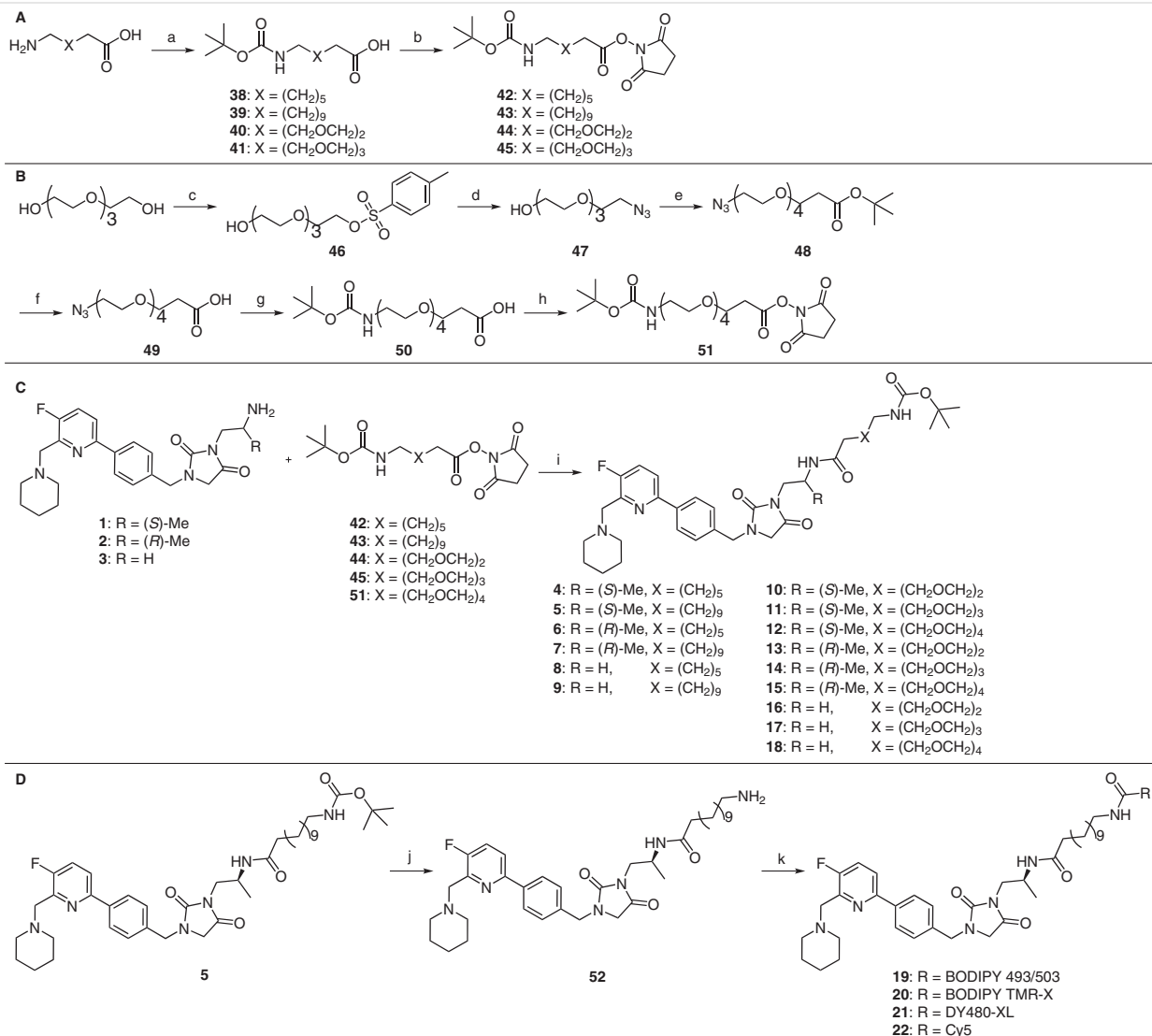


gave iodide derivatives **25** and **26**, respectively. Meanwhile reductive amination of 4-bromobenzaldehyde and aminoacetamide led to compound **27**. After cyclization, the formed imidazolidinedione **28** was alkylated with *tert*-butyl-(2-bromoethyl)carbamate, **25**, or **26** which afforded compounds **29–31**.²⁴ Next, oxidation of 6-bromo-3-fluoro-2-methylpyridine with *m*-CPBA followed by a Boekelheide rearrangement led to **32**. After mesylation of the primary alcohol, the mesyl **33** was substituted with piperidine (**34**). Subsequently, borylation of **29–31** with pinacolboronic ester and conjugation to **34** via a Suzuki coupling gave **35–37**,²⁵ and final acidolysis gained pharmacophores **1–3** (Scheme 2).²⁶

The various alkyl and ethyleneglycol based spacers (**42–45**, **51**) were synthesized according to the generic synthesis depicted in Scheme 3A/B. Alkyl spacers C_8 and C_{12} were synthesized from 8-aminooctanoic acid and 12-aminodecanoic acid, respectively. The glycol spacers PEG2 and PEG3 were synthesized from 3-(2-(2-aminoethoxy)ethoxy)propanoic acid and 3-(2-(2-(2-aminoethoxy)ethoxy)ethoxy)propanoic acid, respectively.

The amino acids were *N*-Boc protected (**38–41**)²⁷ and subsequently converted into the O-Su active esters **42–45**.²⁸ The PEG4 glycol spacer required several additional steps (Scheme 3B). Tsylation of tetraethylene glycol (**46**) was followed by azide substitution (**47**) of the sulfonate ester. This allowed a Michael addition to *tert*-butyl acrylate under TBAF conditions to give **48**. Acidolysis of the ester to give **49** was followed by reduction of the azide and simultaneous *N*-Boc protection to give acid **50**. The last step introduced the *N*-succinimide ester to give **51**.

The three pharmacophores (**1–3**) were conjugated under basic conditions to the five spacers (**42–45**, **51**) to yield 15 CB_2R probe precursors **4–18** (Scheme 3C).²⁹ The most potent of these series, namely compound **5**,³⁰ was *N*-Boc deprotected to give **52**³¹ and thereafter conjugated to the four fluorophores (Scheme 3D), affording the BODIPY 493/503 (**19**), BODIPY TMR-X (**20**), DY480-XL (**21**) and Cy5 (**22**)³² LEI-102 based probes.



Scheme 3 The synthesis of the 15 intermediates followed by the synthesis of the fluorescent probes. *Reagents and conditions:* (a) *Alkyl:* Et₃N (2 equiv), Boc₂O (1.1 equiv), acetone/H₂O (1:1, v/v, 0.5 M), r.t., 16 h, 95–99%; *PEG:* K₂CO₃ (3 equiv), Boc₂O (1.3 equiv), H₂O/THF (1:1, v/v, 0.1 M), r.t., 16 h, 40–81%; (b) *Alkyl:* EDC·HCl (0.8–0.9 equiv), NHS (1.7–2.8 equiv), DCM (0.3 M), r.t., 16–72 h, 36–40%; *PEG:* EDC·HCl (3 equiv), NHS (1.5 equiv), Et₃N (3 equiv), DCM (0.2 M), r.t., 16 h, 46–58%; (c) *p*-TsCl (1 equiv), NaOH (2 M, 1.6 equiv), THF (0.6 M), 0 °C, 4 h, 90%; (d) NaN₃ (1.5 equiv), ACN (0.4 M), 80 °C, 8 h, 94%; (e) *tert*-butyl acrylate (1 equiv), TBAF (0.4 equiv), NaOH (25 wt% in H₂O, 2.6 equiv), DCM, r.t., 8 h, 75%; (f) TFA (50 equiv), DCM, r.t., 4 h, 65%; (g) step 1: 10% Pd/C (0.1 equiv), H₂ gas, EtOH (0.3 M), r.t., 16 h; step 2: K₂CO₃ (3 equiv), Boc₂O (1.3 equiv), H₂O/THF (1:1, v/v, 0.1 M), r.t., 16 h, 55% (two steps); (h) EDC·HCl (1.2 equiv), NHS (1.1 equiv), DCM (0.2 M), r.t., 16 h, 84%; (i) Et₃N (6 equiv), DCM (0.3 M), r.t., 1–3 h, 13–65%; (j) TFA (110 eq), DCM, r.t., 2 h, quant.; (k) **19–21:** Et₃N (1 equiv), fluorophore-NHS ester (1 equiv), CH₂Cl₂ (0.3 M), r.t., 1–3 h, 64–100%; **22:** HOBT (1.2 equiv), DIPEA (2.5 equiv), EDC·HCl (1.3 equiv), cyanine-5-carboxylic acid (1.1 equiv), DMF (0.007 M), r.t., 16 h, quant.

Molecular Pharmacology

Compounds **1–22** were tested at 1 μM in a [³H]CP-55,940 radioligand displacement assay to determine their affinity for the CB₂R and CB₁R. Compounds with less than 50% displacement were considered inactive. The results are shown in Table 1.

Compound **5** was the only scaffold that was active on hCB₂R (63% ± 5 at 1 μM), but not hCB₁R (pK_i < 5), therefore the four fluorophores were only conjugated to this scaffold. Subsequently, the binding affinity (pK_i), potency (pEC₅₀) and efficacy (E_{max}) of compounds **19–22** was determined in a functional [³⁵S]GTPγS assay (Table 1 and Figure 2). Compound **22** displayed a pK_i (CB₂R) of 6.2 ± 0.6 and was inactive on CB₁R. The other fluorescent probes were inactive at

Table 1 hCB₁R and hCB₂R Binding Affinity and Potency of Compounds 1–22^a

Compound	CB ₂ R				CB ₁ R
	Displacement (% ± SEM)	pK _i ± SEM	pEC ₅₀ ± SEM	E _{max} (% ± SEM)	Displacement (% ± SEM)
LEI-102	84 ± 4	8.6 ± 0.3	7.3 ± 0.4	46 ± 17	-20 ± 8
1	35 ± 10	<5	6.4 ± 0.1	28 ± 4	-20 ± 27
2	-4 ± 10	n.d.	n.d.	n.d.	-20 ± 17
3	0 ± 13	n.d.	n.d.	n.d.	-2 ± 18
4	25 ± 9	n.d.	n.d.	n.d.	28 ± 13
5	63 ± 5	6.5 ± 0.1	6.3 ± 0.2	-73 ± 4	36 ± 3
6	22 ± 7	n.d.	n.d.	n.d.	-16 ± 29
7	19 ± 8	n.d.	n.d.	n.d.	30 ± 2
8	27 ± 10	n.d.	n.d.	n.d.	-15 ± 28
9	43 ± 4	n.d.	n.d.	n.d.	32 ± 20
10	-13 ± 22	n.d.	n.d.	n.d.	-17 ± 24
11	-4 ± 4	n.d.	n.d.	n.d.	-22 ± 14
12	11 ± 21	n.d.	n.d.	n.d.	1 ± 12
13	-12 ± 15	n.d.	n.d.	n.d.	5 ± 10
14	3 ± 1	n.d.	n.d.	n.d.	-3 ± 15
15	1 ± 19	n.d.	n.d.	n.d.	-2 ± 10
16	-7 ± 16	n.d.	n.d.	n.d.	0 ± 16
17	1 ± 10	n.d.	n.d.	n.d.	5 ± 19
18	15 ± 14	n.d.	n.d.	n.d.	7 ± 16
19	31 ± 3	<5	n.d.	n.d.	-12 ± 6
20	16 ± 4	<5	n.d.	n.d.	-63 ± 37
21	17 ± 14	<5	n.d.	n.d.	-16 ± 19
22	39 ± 5	6.2 ± 0.6	5.3 ± 0.1	-63 ± 6	10 ± 18

^a Binding affinities were determined either as displacement (%) or pK_i using a [³H]CP-55,940 radioligand displacement assay on CHO cells stably over-expressing either hCB₂R_{bgal} or hCB₁R_{bgal}. The displacement percentages represent the percentage of radioligand displaced from the receptor at 1 μM compound. Total binding at vehicle concentration was set at 0%, while non-specific binding was set at 100%. Potency values (pEC₅₀) were obtained for compounds with displacement ≥35% using a [³⁵S]GTPγS assay on CHO cells stably over-expressing hCB₂R_{bgal}. The maximum effect (E_{max} in %) was normalized to reference full agonist CP-55,940. All values are presented as the mean ± SEM of at least two independent experiments performed in triplicate. n.d. not determined.

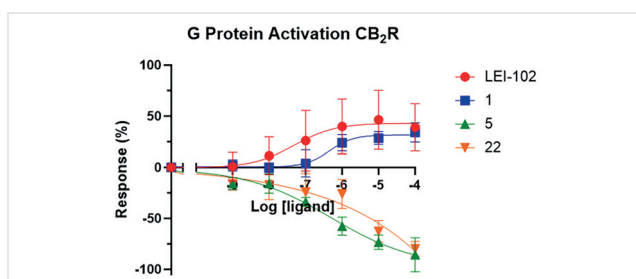


Figure 2 G protein activation levels on CB₂R were determined with a [³⁵S]GTPγS assay. Basal activity in the presence of vehicle was set to 0%, whereas full G protein activation was determined using 10 μM of full agonist CP-55,940 and was set as 100%. Data are expressed as mean ± SEM from three experiments performed in triplicate.

CB₂R. In contrast to LEI-102 and the parent compound **1**, compound **22** was an inverse agonist with a pEC₅₀ of 5.3 ± 0.1 and E_{max} of -63% ± 6. Previously, we have noted that

very small structural changes in a compound may change the functional behavior of the CB₂R.¹⁵ It is not clear from a structural point of view what is the cause of this switch in functionality. We speculate that the alkyl linker may prevent the conformational change needed by one or more of the seven transmembrane helices in the binding site to activate the receptor.

A structure-based approach in combination with rational design was used to develop a one-step fluorescent probe for the cannabinoid CB₂ receptor based on a pyridin-2-yl-benzyl-imidazolidine-2,4-dione scaffold. Ultimately probe **22** was synthesized with an alkyl spacer and Cy5 fluorescent dye. Probe **22** demonstrated reasonable CB₂R affinity (pK_i 6.2 ± 0.6), was selective over CB₁R, and behaved as an inverse agonist (EC₅₀ 5.3 ± 0.1, E_{max} -63% ± 6). It is envisioned that probe **22** can be used to visualize CB₂R in cells without the need for copper-assisted click reactions.

Author Contributions

Design: A.P.A.J. (Antonius P.A. Janssen), A.H. (Asad Halimi), L.V.d.P. (Laura V. de Paus); Conducting Experiments, A.H., L.V.d.P.; Writing-Original Draft, L.V.d.P.; Writing Review & Editing, M.v.d.S., L.H.H. (Laura H. Heitman), R.J.B.H.N.v.d.B (Richard J. B. H. N. van den Berg).

Conflict of Interest

The authors declare no conflict of interest.

Funding Information

This work was supported by the Dutch Research Council (Nederlandse Organisatie voor Wetenschappelijk Onderzoek; NWO, Navistroke #15851).

Supporting Information

Supporting information for this article is available online at <https://doi.org/10.1055/a-2230-1003>.

References

- Mallipeddi, S.; Janero, D. R.; Zvonok, N.; Makriyannis, A. *Biochem. Pharmacol.* **2017**, *128*, 1; <https://doi.org/10.1016/j.bcp.2016.11.014>.
- Basagni, F.; Rosini, M.; Decker, M. *ChemMedChem* **2020**, *15*, 1374; <https://doi.org/10.1002/cmcd.202000298>.
- Hamilton, A. J.; Payne, A. D.; Mocerino, M.; Gunosewoyo, H. *Aust. J. Chem.* **2021**, *74*, 416; <https://doi.org/10.1071/CH21007>.
- Spinelli, F.; Giampietro, R.; Stefanachi, A.; Riganti, C.; Kopecka, J.; Abatematteo, F. S.; Leonetti, F.; Colabufo, N. A.; Mangiatordi, G. F.; Nicolotti, O.; Perrone, M. G.; Brea, J.; Loza, M. I.; Infantino, V.; Abate, C.; Contino, M. *Eur. J. Med. Chem.* **2020**, *188*, 112037; <https://doi.org/10.1016/j.ejmech.2020.112037>.
- Ling, X.; Zhang, S.; Liu, Y.; Bai, M. *J. Biomed. Opt.* **2018**, *23*, 1; <https://doi.org/10.1117/1.JBO.23.10.108001>.
- Zhang, S.; Shao, P.; Bai, M. *Bioconjugate Chem.* **2013**, *24*, 1907; <https://doi.org/10.1021/bc400328m>.
- Singh, S.; Oyagawa, C. R. M. M.; Macdonald, C.; Grimsey, N. L.; Glass, M.; Vernall, A. J. *ACS Med. Chem. Lett.* **2019**, *10*, 209; <https://doi.org/10.1021/acsmchemlett.8b00597>.
- Martín-Couce, L.; Martín-Fontecha, M.; Palomares, Ó.; Mestre, L.; Cordero, A.; Hernangomez, M.; Palma, S.; Pardo, L.; Guaza, C.; López-Rodríguez, M. L.; Ortega-Gutiérrez, S. *Angew. Chem. Int. Ed.* **2012**, *51*, 6896; <https://doi.org/10.1002/anie.201200467>.
- Martín-Fontecha, M.; Angelina, A.; Rückert, B.; Rueda-Zubiurre, A.; Martín-Cruz, L.; van de Veen, W.; Akdis, M.; Ortega-Gutiérrez, S.; López-Rodríguez, M. L.; Akdis, C. A.; Palomares, O. *Bioconjugate Chem.* **2018**, *29*, 382; <https://doi.org/10.1021/acs.bioconjchem.7b00680>.
- Sarott, R. C.; Viray, A. E. G.; Pfaff, P.; Sadybekov, A.; Rajic, G.; Katritch, V.; Carreira, E. M.; Frank, J. A. *J. Am. Chem. Soc.* **2021**, *143*, 736; <https://doi.org/10.1021/jacs.0c08926>.
- Cooper, A. G.; Oyagawa, C. R. M.; Manning, J. J.; Singh, S.; Hook, S.; Grimsey, N. L.; Glass, M.; Tyndall, J. D. A.; Vernall, A. *J. Med. Chem. Comm.* **2018**, *9*, 2055; <https://doi.org/10.1039/C8MD00448J>.
- Sarott, R. C.; Westphal, M. V.; Pfaff, P.; Korn, C.; Sykes, D. A.; Gazzi, T.; Brennecke, B.; Atz, K.; Weise, M.; Mostinski, Y.; Hompluem, P.; Miljuš, T.; Roth, N. J.; Asmelash, H.; Vong, M. C.; Piovesan, J.; Guba, W.; Rufer, A. C.; Kuznir, E. A.; Huber, S.; Raposo, C.; Zirwes, E. A.; Osterwald, A.; Pavlovic, A.; Moes, S.; Beck, J.; Benito-Cuesta, I.; Grande, T.; Yeliseev, A.; Drawnel, F.; Widmer, G.; Holzer, D.; Van Der Wel, T.; Mandhair, H.; Yuan, C.-Y.; Drobyski, W. R.; Saroz, Y.; Grimsey, N.; Honer, M.; Fingerle, J.; Gawrisch, K.; Romero, J.; Hillard, C. J.; Varga, Z. V.; Van Der Stelt, M.; Pacher, P.; Gertsch, J.; McCormick, P. J.; Ullmer, C.; Oddi, S.; Maccarrone, M.; Veprintsev, D. B.; Nazaré, M.; Grether, U.; Carreira, E. M. *ChemRxiv* **2019**, preprint DOI: 10.26434/chemrxiv.10288547.v1.
- Sarott, R. C.; Westphal, M. V.; Pfaff, P.; Korn, C.; Sykes, D. A.; Gazzi, T.; Brennecke, B.; Atz, K.; Weise, M.; Mostinski, Y.; Hompluem, P.; Koers, E.; Miljuš, T.; Roth, N. J.; Asmelash, H.; Vong, M. C.; Piovesan, J.; Guba, W.; Rufer, A. C.; Kuznir, E. A.; Huber, S.; Raposo, C.; Zirwes, E. A.; Osterwald, A.; Pavlovic, A.; Moes, S.; Beck, J.; Benito-Cuesta, I.; Grande, T.; Ruiz de Martín Esteban, S.; Yeliseev, A.; Drawnel, F.; Widmer, G.; Holzer, D.; van der Wel, T.; Mandhair, H.; Yuan, C.-Y.; Drobyski, W. R.; Saroz, Y.; Grimsey, N.; Honer, M.; Fingerle, J.; Gawrisch, K.; Romero, J.; Hillard, C. J.; Varga, Z. V.; van der Stelt, M.; Pacher, P.; Gertsch, J.; McCormick, P. J.; Ullmer, C.; Oddi, S.; Maccarrone, M.; Veprintsev, D. B.; Nazaré, M.; Grether, U.; Carreira, E. M. *J. Am. Chem. Soc.* **2020**, *142*, 16953; <https://doi.org/10.1021/jacs.0c05587>.
- Gazzi, T.; Brennecke, B.; Atz, K.; Korn, C.; Sykes, D.; Forn-Cuni, G.; Pfaff, P.; Sarott, R. C.; Westphal, M. V.; Mostinski, Y.; Mach, L.; Wasinska-Kalwa, M.; Weise, M.; Hoare, B. L.; Miljuš, T.; Mexi, M.; Roth, N.; Koers, E. J.; Guba, W.; Alker, A.; Rufer, A. C.; Kuznir, E. A.; Huber, S.; Raposo, C.; Zirwes, E. A.; Osterwald, A.; Pavlovic, A.; Moes, S.; Beck, J.; Nettekoven, M.; Benito-Cuesta, I.; Grande, T.; Drawnel, F.; Widmer, G.; Holzer, D.; van der Wel, T.; Mandhair, H.; Honer, M.; Fingerle, J.; Scheffel, J.; Broichhagen, J.; Gawrisch, K.; Romero, J.; Hillard, C. J.; Varga, Z. V.; van der Stelt, M.; Pacher, P.; Gertsch, J.; Ullmer, C.; McCormick, P. J.; Oddi, S.; Spaink, H. P.; Maccarrone, M.; Veprintsev, D. B.; Carreira, E. M.; Grether, U.; Nazaré, M. *Chem. Chem. Sci.* **2022**, *13*, 5539; <https://doi.org/10.1039/D1SC06659E>.
- Soethoudt, M.; Stolze, S. C.; Westphal, M. V.; van Stralen, L.; Martella, A.; van Rooden, E. J.; Guba, W.; Varga, Z. V.; Deng, H.; van Kasteren, S. I.; Grether, U.; IJzerman, A. P.; Pacher, P.; Carreira, E. M.; Overkleef, H. S.; Ioan-Facsinay, A.; Heitman, L. H.; van der Stelt, M. *J. Am. Chem. Soc.* **2018**, *140*, 6067; <https://doi.org/10.1021/jacs.7b11281>.
- Li, X.; Chang, H.; Bouma, J.; de bPaus, L. V.; Mukhopadhyay, P.; Paloczi, J.; Mustafa, M.; van der Horst, C.; Kumar, S. S.; Wu, L.; Yu, Y.; van den Berg, R. J. B. H. N.; Janssen, A. P. A.; Lichtman, A.; Liu, Z.-J.; Pacher, P.; van der Stelt, M.; Heitman, L. H.; Hua, T. *Nat. Commun.* **2023**, *14*, 1447; <https://doi.org/10.1038/s41467-023-7112-9>.
- Loudet, A.; Burgess, K. *Chem. Rev.* **2007**, *107*, 4891; <https://doi.org/10.1021/cr078381n>.
- Deng, Y.; Cheng, Y.; Liu, H.; Mack, J.; Lu, H.; Zhu, L. *Tetrahedron Lett.* **2014**, *55*, 3792; <https://doi.org/10.1016/j.tetlet.2014.05.066>.
- Widengren, J.; Schwille, P. *J. Phys. Chem. A* **2000**, *104*, 6416; <https://doi.org/10.1021/jp000059s>.
- Buschmann, V.; Weston, K. D.; Sauer, M. *Bioconjugate Chem.* **2003**, *14*, 195; <https://doi.org/10.1021/bc025600x>.
- Olympus Life Sciences., *Fluorophores for Confocal Microscopy*. <https://www.olympus-lifescience.com/en/microscope-resource/primer/techniques/confocal/fluorophoresintro/> (accessed 2020-04-15).

- (22) Gao, Z.; Hao, Y.; Zheng, M.; Chen, Y. *RSC Adv.* **2017**, *7*, 7604; <https://doi.org/10.1039/C6RA27547H>.
- (23) **General Procedure:** All reagents and solvents were purchased from commercial sources and were of analytical grade. Reagents and solvents were not further purified before use. All moisture-sensitive reactions were performed under inert atmosphere. Solvents were dried using 4Å molecular sieves prior to use when anhydrous conditions were required. Water used in reactions was always demineralized. Analytical thin-layer chromatography (TLC) was routinely performed to monitor the progression of a reaction and was conducted on silica gel 60 F254 plates. Reaction compounds on the TLC plates were visualized by UV irradiation (λ_{254}) and/or spraying with potassium permanganate solution (K_2CO_3 (40 g), $KMnO_4$ (6 g), and H_2O (600 mL)), ninhydrin solution (ninhydrin (1.5 g), n-butanol (100 mL) and acetic acid (3.0 mL)) or molybdenum solution ($(NH_4)_6MO_7O_{24} \cdot 4H_2O$ (25 g/L) and $(NH_4)_4Ce(SO_4)_4 \cdot 2H_2O$ (10 g/L) in sulfuric acid (10%)) followed by heating as appropriate. Purification by flash column chromatography was performed using silica gel 60 (40–63 μ m, pore diameter of 60Å). Solutions were concentrated using a rotary evaporator.
- (24) **Preparation of 29:** A mixture of **28** (2.70 g, 10.0 mmol, 1 equiv), **25** (5.72 g, 20.1 mmol, 2 equiv), K_2CO_3 (8.32 g, 60.2 mmol, 6 equiv) and 18-crown-6 (0.53 g, 2.0 mmol, 0.2 equiv) in DMF (55 mL) was heated (50 °C) overnight. After cooling to r.t., the mixture was diluted with H_2O (40 mL) and Et_2O (40 mL). The layers were separated and the aqueous layer was extracted thrice with Et_2O . The combined organic layer was washed five times with H_2O and once with brine, dried ($MgSO_4$), filtered, and the solvent evaporated under reduced pressure. The crude product was purified with flash column chromatography (SiO_2 , 20–50% EtOAc in pentane) to yield the product (2.67 g, 6.3 mmol, 62%) as a yellow solid. 1H NMR (850 MHz, $CDCl_3$): δ = 7.48 (d, J = 8.4 Hz, 2 H), 7.18 (d, J = 8.1 Hz, 2 H), 4.71–4.67 (m, 2 H), 4.34 (d, J = 15.3 Hz, 1 H), 4.06 (hept, J = 6.5 Hz, 1 H), 3.72 (d, J = 17.1 Hz, 1 H), 3.66 (d, J = 17.2 Hz, 1 H), 3.51 (d, J = 7.9 Hz, 2 H), 1.37 (s, 9 H), 1.17 (d, J = 6.8 Hz, 3 H). ^{13}C NMR (214 MHz, $CDCl_3$): δ = 170.11, 157.03, 155.73, 134.58, 132.24, 129.93, 122.26, 79.32, 49.10, 46.16, 45.52, 44.97, 28.41, 18.63. LC-MS (ESI, 10–90): t_R = 7.64 min; m/z = 425.53 $[M + H]^+$.
- (25) **Preparation of 35:** A stirred and degassed mixture of **29** (2.67 g, 6.3 mmol, 1.1 equiv), $Pd(dppf)Cl_2$ (0.24 g, 0.3 mmol, 0.05 equiv), bis(pinacolato)diboron (2.40 g, 9.5 mmol, 1.5 equiv) and KOAc (2.70 g, 27.5 mmol, 4.4 equiv) in DMF (30 mL) was heated (75 °C) overnight. The reaction was diluted at r.t. with H_2O and EtOAc. The layers were separated and the aqueous layer extracted thrice with EtOAc. The combined organic layer was washed with sat. $NaHCO_3$ (aq), H_2O , and brine, dried ($MgSO_4$), filtered and the solvent evaporated under reduced pressure. The crude residue was used without further purification. The crude residue was co-evaporated thrice with chloroform and re-dissolved in degassed toluene/EtOH (30 mL, 4:1, v/v). To the stirred mixture was added **34** (1.64 g, 6.0 mmol, 1 equiv), K_2CO_3 (3.46 g, 25.0 mmol, 4 equiv) and $Pd(PPh_3)_4$ (0.50 g, 0.4 mmol, 0.06 equiv). After heating (75 °C) overnight, the reaction was diluted at r.t. with H_2O and EtOAc. The layers were separated and the aqueous layer was extracted thrice with EtOAc. The combined organic layer was washed with H_2O and brine, dried ($MgSO_4$), filtered and the solvent evaporated under reduced pressure. The crude product was purified with flash column chromatography (SiO_2 , 0–4% MeOH in DCM) to yield a brown oil (1.40 g, 2.6 mmol, 42%). 1H NMR (400 MHz, $CDCl_3$): δ = 7.94 (d, J = 8.3 Hz, 2 H), 7.60 (dd, J = 8.6, 3.5 Hz, 1 H), 7.41 (t, J = 8.8 Hz, 1 H), 7.35 (d, J = 7.9 Hz, 2 H), 4.82–4.68 (m, 2 H), 4.47 (d, J = 15.2 Hz, 1 H), 4.05 (p, J = 7.1 Hz, 1 H), 3.82 (d, J = 2.7 Hz, 2 H), 3.72 (d, J = 8.8 Hz, 2 H), 3.52 (d, J = 6.6 Hz, 2 H), 2.62–2.55 (m, 4 H), 1.59 (p, J = 5.7 Hz, 4 H), 1.38 (s, 11 H), 1.17 (d, J = 6.7 Hz, 3 H). ^{13}C NMR (101 MHz, $CDCl_3$): δ = 170.27, 157.94 (d, J = 258.1 Hz), 157.06, 155.71, 151.88 (d, J = 4.9 Hz), 145.63 (d, J = 15.1 Hz), 138.62, 135.95, 128.59, 127.61, 127.55, 123.70 (d, J = 20.4 Hz), 120.39 (d, J = 4.1 Hz), 79.26, 58.44 (d, J = 3.0 Hz), 54.36, 49.10, 46.49, 45.60, 44.80, 28.43, 25.98, 24.18, 18.62. LC-MS (ESI, 10–90): t_R = 5.47 min; m/z = 540.20 $[M + H]^+$.
- (26) **Preparation of 1:** To a solution of **35** (1.40 g, 2.6 mmol, 1 equiv) in ACN (5 mL) was added 4 M HCl in 1,4-dioxane (2.7 mL, 10.8 mmol, 4.1 equiv). After the reaction was heated (80 °C) for 2 h, the ACN was evaporated under reduced pressure. The mixture was basified with 1 M NaOH (aq) until pH 10. The aqueous layer was extracted with $CHCl_3/MeOH$ (7:1, v/v). NaCl was added for increased separation. The combined organic layer was dried ($MgSO_4$), filtered, and the solvent evaporated under reduced pressure. The crude product was purified with flash column chromatography (SiO_2 , 0–4% MeOH in DCM with 2% Et_3N (v/v)) to yield the product (0.98 g, 2.2 mmol, 86%) as an orange oil. 1H NMR (400 MHz, $CDCl_3$): δ = 7.96 (d, J = 8.2 Hz, 2 H), 7.62 (dd, J = 8.6, 3.5 Hz, 1 H), 7.42 (t, J = 8.8 Hz, 1 H), 7.34 (d, J = 8.3 Hz, 2 H), 4.61 (s, 2 H), 3.83 (d, J = 2.7 Hz, 2 H), 3.78 (s, 2 H), 3.54–3.38 (m, 2 H), 3.32–3.19 (m, 1 H), 2.59 (s, 4 H), 1.60 (p, J = 5.6 Hz, 6 H), 1.46–1.36 (m, 2 H), 1.13 (d, J = 6.4 Hz, 3 H). ^{13}C NMR (101 MHz, $CDCl_3$): δ = 170.35, 157.98 (d, J = 258.1 Hz), 157.25, 151.84 (d, J = 4.9 Hz), 145.80 (d, J = 15.0 Hz), 138.79, 135.92, 128.66, 127.63, 123.73 (d, J = 20.4 Hz), 120.43 (d, J = 4.2 Hz), 58.55 (d, J = 3.2 Hz), 54.45, 49.15, 47.19, 46.61, 46.21, 26.06, 24.23, 22.10. LC-MS (ESI, 10–90): t_R = 3.74 min; m/z = 440.33 $[M + H]^+$. HRMS: m/z calcd for $[C_{24}H_{30}FN_3O_2 + H]^+$: 440.24563; found: 440.24533.
- (27) **Preparation of 39:** To a cooled (0 °C) and stirred mixture of 12-aminododecanoic acid (1.50 g, 7.0 mmol, 1 equiv) and Et_3N (1.9 mL, 13.9 mmol, 2 equiv) in acetone/ H_2O (14 mL, 1:1, v/v) was added dropwise Boc_2O (1.67 g, 7.7 mmol, 1.1 equiv) in acetone (4 mL). After stirring at r.t. overnight, the acetone was evaporated under reduced pressure. The aqueous layer was acidified with 1 M HCl to pH 4 before being extracted thrice with EtOAc. The combined organic layer was washed with brine, dried ($MgSO_4$), and filtered. The solvent was evaporated under reduced pressure to yield the product (2.09 g, 6.6 mmol, 95%) as a white solid. 1H NMR (400 MHz, $CDCl_3$): δ = 4.54 (s, 1 H), 3.10 (m, 2 H), 2.34 (t, J = 7.4 Hz, 2 H), 1.63 (p, J = 7.4 Hz, 2 H), 1.51–1.40 (m, 11 H), 1.38–1.21 (m, 14 H). ^{13}C NMR (101 MHz, $CDCl_3$): δ = 179.28, 156.27, 79.12, 40.64, 33.98, 30.02, 29.44, 29.42, 29.34, 29.24, 29.18, 29.02, 28.44, 26.78, 24.69. LC-MS (ESI, 10–90): t_R = 8.44 min; m/z = 315.60 $[M + H]^+$.
- (28) **Preparation of 43:** To a stirred solution of **39** (2.09 g, 6.6 mmol, 1.3 equiv) in DCM (35 mL) was added EDC-HCl (0.99 g, 5.2 mmol, 1 equiv) and *N*-hydroxysuccinimide (1.66 g, 14.4 mmol, 2.8 equiv). After stirring at r.t. for 3 days, the reaction was quenched with sat. NH_4Cl (aq). The layers were separated and the aqueous layer was extracted once with DCM. The combined organic layer was dried ($MgSO_4$), filtered, and the solvent evaporated under reduced pressure. The crude product was purified with flash column chromatography (SiO_2 , 10–40% EtOAc in pentane) to yield the product (0.88 g, 2.1 mmol, 40%) as a white solid. 1H NMR (400 MHz, $CDCl_3$): δ = 4.54 (s, 1 H), 3.12 (q, J = 6.8 Hz, 2 H), 2.86 (d, J = 4.3 Hz, 4 H), 2.62 (t, J = 7.5 Hz, 2 H), 1.76 (p, J = 7.4 Hz, 2 H), 1.50–1.42 (m, 11 H), 1.35–1.25 (m, 14 H). ^{13}C NMR (101 MHz, $CDCl_3$): δ = 169.34, 168.83, 165.27, 156.11,

79.12, 40.76, 31.07, 30.18, 29.61, 29.54, 29.41, 29.39, 29.17, 28.88, 28.56, 26.92, 25.72, 24.69. LC-MS (ESI, 10-90): $t_R = 8.87$ min; $m/z = 412.60$ [M]⁺.

(29) **General preparation of Key Intermediates KI (4-18):** A mixture of **1**, **2** or **3** (1 equiv), Et₃N (6 equiv) and *O*-Su ester (**42**, **43**, **44**, **45** or **51**, 1 equiv) in DCM (0.3 M) was stirred at r.t. for 1–3 h. The reaction mixture was diluted with H₂O and DCM. The layers were separated and the aqueous layer was extracted thrice with DCM. The combined organic layer was washed with H₂O and brine, dried (MgSO₄), filtered, and the solvent evaporated under reduced pressure. The crude product was purified using preparative HPLC and freeze-dried twice.

(30) **Preparation of 5:** Compound **5** was synthesized according to general preparation KI²⁹ using **1** (92.0 mg, 21.0 μmol, 1 equiv) and **43** (87.0 mg, 21.0 μmol, 1 equiv). The product was obtained as a white solid (75.2 mg, 0.10 mmol, 49%). ¹H NMR (400 MHz, CDCl₃): δ = 7.97 (d, *J* = 8.0 Hz, 2 H), 7.63 (dd, *J* = 8.6, 3.5 Hz, 1 H), 7.43 (t, *J* = 8.8 Hz, 1 H), 7.34 (d, *J* = 8.0 Hz, 2 H), 6.00 (d, *J* = 8.1 Hz, 1 H), 4.62 (s, 2 H), 4.54 (s, 1 H), 4.39–4.24 (m, 1 H), 3.86 (d, *J* = 2.5 Hz, 2 H), 3.76 (q, *J* = 17.3 Hz, 2 H), 3.64–3.51 (m, 2 H), 3.09 (q, *J* = 6.7 Hz, 2 H), 2.62 (s, 4 H), 2.11 (t, *J* = 7.6 Hz, 2 H), 1.66–1.54 (m, 6 H), 1.44 (s, 13 H), 1.34–1.23 (m, 14 H), 1.19 (d, *J* = 6.7 Hz, 3 H). ¹³C NMR (101 MHz, CDCl₃): δ = 173.25, 170.39, 158.01 (d, *J* = 258.3 Hz), 157.26, 151.82, 138.76, 135.80, 128.55, 127.65, 123.75 (d, *J* = 20.2 Hz), 120.46, 77.48, 77.16, 76.84, 58.34, 54.31, 49.22, 46.60, 45.07, 44.23, 40.77, 37.03, 30.19, 29.64, 29.58, 29.47, 29.41, 28.57, 26.93, 25.95, 25.70, 24.19, 18.45. LC-MS (ESI, 10-90): $t_R = 7.10$ min; $m/z = 737.33$ [M + H]⁺. HRMS: m/z calcd for [C₄₁H₆₁FN₆O₅ + H]⁺: 737.47602; found: 737.47562.

(31) **Preparation of 52:** A mixture of **5** (435 mg, 0.6 mmol, 1 equiv) and TFA (5 mL, 64.9 mmol, 110 equiv) in DCM (10 mL) was stirred at r.t. for 2 h. The volatile compounds were evaporated under reduced pressure. The crude was re-dissolved in DCM and 1 M (aq) NaOH was added until pH 10. The layers were separated and the aqueous layer extracted thrice with chloroform. The combined organic layer was dried (MgSO₄), filtered and the solvent evaporated under reduced pressure to yield the product (376 mg, 0.59 mmol, quant.) as a yellow oil. ¹H NMR (500 MHz, CDCl₃): δ = 7.94 (d, *J* = 8.3 Hz, 2 H), 7.60 (dd, *J* = 8.6, 3.5 Hz, 1 H), 7.41 (t, *J* = 8.8 Hz, 1 H), 7.33 (d, *J* = 8.3 Hz, 2 H), 6.09 (d, *J* = 8.1 Hz, 1 H), 4.60 (s, 2 H), 4.35–4.25 (m, 1 H), 3.81 (d, *J* = 2.6 Hz, 2 H), 3.75 (q, *J* = 17.5 Hz, 2 H), 3.62–3.49 (m, 2 H), 2.74 (t, *J* = 7.5 Hz, 2 H), 2.58 (s, 4 H), 2.10 (t, *J* = 7.5 Hz, 2 H), 1.59 (p, *J* = 5.6 Hz, 4 H), 1.56–1.46 (m, 2 H), 1.44–1.37 (m, 2 H), 1.29–1.18 (m, 16 H),

1.17 (d, *J* = 6.7 Hz, 3 H). ¹³C NMR (126 MHz, CDCl₃): δ = 173.48, 170.46, 162.32, 162.05, 157.93 (d, *J* = 258.3 Hz), 157.21, 156.90, 151.95 (d, *J* = 5.0 Hz), 145.52 (d, *J* = 15.1 Hz), 138.63, 135.82, 128.52, 127.58, 123.78 (d, *J* = 20.2 Hz), 120.56 (d, *J* = 5.0 Hz), 58.29 (d, *J* = 2.5 Hz), 54.37, 53.54, 50.57, 49.19, 46.49, 44.78, 44.18, 40.98, 36.86, 30.40, 29.40, 29.36, 29.27, 29.24, 29.18, 28.92, 28.82, 26.63, 25.88, 25.60, 24.13, 18.27. LC-MS (ESI, 10-90): $t_R = 4.84$ min; $m/z = 637.53$ [M + H]⁺.

(32) **Preparation of Cy5 Probe 22:** To a stirred and cooled (0 °C) mixture of cyanine-5-carboxylic acid (23.4 g, 48.4 μmol, 1.1 equiv) in DMF (7 mL) was added HOBt (8.09 mg, 52.8 μmol, 1.2 equiv), **52** (26.94 mg, 42.4 μmol, 1 equiv), DIPEA (18.4 μL, 105.6 μmol, 2.5 equiv) and EDC·HCl (9.69 mg, 50.5 μmol, 1.2 equiv). After stirring overnight at r.t., H₂O (7 mL) and EtOAc (7 mL) was added. The layers were separated and the aqueous layer extracted thrice with EtOAc. The combined organic layer was washed with sat (aq) NaHCO₃, five times with H₂O, and once with brine, dried (MgSO₄), filtered, and the solvent evaporated under reduced pressure. The crude product was purified with preparative HPLC and freeze-dried twice to yield the product (50.4 mg, 45.8 μmol, quant.) as a blue solid. ¹H NMR (400 MHz, CDCl₃): δ = 8.02–7.88 (m, 3 H), 7.67 (t, *J* = 5.7 Hz, 1 H), 7.61 (dd, *J* = 8.6, 3.5 Hz, 1 H), 7.41 (t, *J* = 8.8 Hz, 1 H), 7.38–7.29 (m, 6 H), 7.20 (dt, *J* = 11.9, 7.4 Hz, 2 H), 7.08 (dd, *J* = 17.4, 7.9 Hz, 2 H), 6.91 (t, *J* = 12.5 Hz, 1 H), 6.56 (d, *J* = 13.7 Hz, 1 H), 6.27 (d, *J* = 13.5 Hz, 1 H), 6.12 (d, *J* = 8.0 Hz, 1 H), 4.60 (s, 2 H), 4.35–4.23 (m, 1 H), 4.07 (t, *J* = 7.7 Hz, 2 H), 3.81 (d, *J* = 2.6 Hz, 2 H), 3.73 (q, *J* = 17.4 Hz, 2 H), 3.64–3.50 (m, 4 H), 3.19 (q, *J* = 6.4 Hz, 2 H), 2.57 (s, 4 H), 2.35 (t, *J* = 7.2 Hz, 2 H), 2.09 (t, *J* = 7.8 Hz, 2 H), 1.88–1.73 (m, 2 H), 1.70 (s, 6 H), 1.69 (s, 6 H), 1.61–1.48 (m, 10 H), 1.39 (q, *J* = 6.2 Hz, 2 H), 1.29–1.19 (m, 18 H), 1.16 (d, *J* = 6.7 Hz, 3 H). ¹³C NMR (101 MHz, CDCl₃): δ = 173.51, 173.48, 173.25, 172.57, 170.39, 157.93 (d, *J* = 258.0 Hz), 157.22, 154.02, 152.97, 151.77 (d, *J* = 4.9 Hz), 145.79 (d, *J* = 15.0 Hz), 142.94, 142.03, 141.33, 140.76, 138.70, 135.81, 128.88, 128.73, 128.53, 127.59, 126.90, 125.49, 124.94, 123.69 (d, *J* = 20.4 Hz), 122.28, 122.20, 120.38 (d, *J* = 4.2 Hz), 111.03, 110.22, 104.93, 103.65, 58.55 (d, *J* = 3.1 Hz), 54.36, 49.50, 49.20, 49.05, 46.53, 45.01, 44.71, 44.16, 39.67, 36.96, 36.21, 29.80, 29.70, 29.65, 29.62, 29.54, 29.45, 29.40, 29.35, 28.16, 27.23, 27.10, 26.51, 26.06, 25.67, 25.34, 24.22, 18.39. LC-MS (ESI, 10-90): $t_R = 7.36$ min; $m/z = 1101.73$ [M]⁺. HRMS: m/z calcd for [C₆₈H₉₀FN₈O₄ + H]⁺: 1101.70636; found: 1101.70696.